Steady-state dark photorefractive screening solitons

Zhigang Chen, Matthew Mitchell, Ming-feng Shih, and Mordechai Segev

Department of Electrical Engineering and Center for Photonics and Optoelectronic Materials, Princeton University, Princeton, New Jersey 08544

Mark H. Garrett

Deltronic Crystal Industries, Dover, New Jersey 07801

George C. Valley

Hughes Research Laboratories, Malibu, California 90265

Received October 23, 1995

We present an experimental study of steady-state dark photorefractive screening solitons trapped in a bulk strontium barium niobate crystal. We compare experimental measurements with theoretical calculations of the soliton properties and find good agreement between theory and experiments. We confirm the shape-preserving behavior of the dark soliton by measuring its beam profile as it propagates throughout a specially cut crystal and by guiding a beam of a different wavelength.

Since the prediction[1] and experimental observation[2] of photorefractive solitons, their existence at low power and in both transverse dimensions has attracted much fundamental interest, driven also by potential applications such as beam steering, optical interconnects, and nonlinear-optical devices.[1–11] Photorefractive solitons appear in several forms: quasi-steady-state solitons[1,2] and steady-state (screening) solitons,[3–6] both with applied electric field, and photovoltaic solitons.[7,8] Dark photorefractive solitons were first observed in quasi-steady state[9] (along with vortex solitons). Dark screening solitons[4,5] and photovoltaic solitons[7] were predicted shortly thereafter. Recently, dark screening solitons[10] and dark photovoltaic solitons[8] were observed.

We can best understand dark screening solitons by considering a narrow dark notch on an otherwise uniform light beam propagating in a biased photorefractive medium.[4] In the illuminated regions the conductivity increases and the resistivity decreases. Therefore the voltage drops mostly in the dark region, and this leads to a large space-charge field around the notch. The index perturbation is proportional to the space-charge field (through the Pockels effect) and acts as a self-defocusing medium for the illuminated portions of the beam. Consequently these illuminated portions expand their inner boundaries, compensating for the divergence of the notch, thus generating a dark soliton. Note that a dark photorefractive soliton not only confines the dark notch but also induces an effective graded-index waveguide that can guide other beams.[11]

Here we study dark steady-state screening solitons trapped in a bulk strontium barium niobate (SBN) crystal. We use a specially cut crystal to measure the beam profiles of the dark soliton as it propagates throughout the crystal and show that it is indeed solitary-wave propagation. Then we make detailed comparisons between theory and experiment. The theory predicts a universal relation between the soliton width and the ratio of the soliton peak irradiance to the sum of the dark irradiance and a uniform background irradiance.[4,5] For screening solitons the only parameter needed for comparing theory and experiments is V_π, i.e., the voltage necessary for polarization rotation by π, which can be measured separately. We investigate this relation and show good agreement with the measurements with no fitting parameters. Finally, we use the steady-state dark soliton to guide a beam of a different wavelength.

Previous research[4,5] showed that a one-dimensional dark screening soliton is described by the reduced wave equation

$$\mathrm{d}^2u/\mathrm{d}\xi^2 - [1 - (1 + u_\infty^2)/(1 + u^2)]u = 0\,, \qquad (1)$$

where $u(x)$ is the soliton amplitude (as a function of the transverse coordinate x) divided by the square root of the sum of the background and dark irradiances, u_∞ is the (maximum) soliton amplitude at $x = \ell/2$, and $\xi = x/d$, where $d = (k^2 n_b^2 r_{\mathrm{eff}} V/\ell)^{-1/2}$; $k = 2\pi n_b/\lambda$, λ is the free-space wavelength, n_b is the unperturbed refractive index, r_{eff} is the effective electro-optic coefficient for the geometry of propagation, V is the applied voltage, and ℓ is the width of the crystal between the electrodes. The boundary conditions for dark-soliton solutions of Eq. (1) are $u(0) = 0$ and $\mathrm{d}u/\mathrm{d}\xi(0) = [(1 + u_\infty^2)\ln(1 + u_\infty^2) - u_\infty^2]$. Equation (1) can be integrated numerically to yield the spatial profile of the soliton and the FWHM of the intensity as a function of u_∞. The solution of Eq. (1) predicts that the soliton width as a function of u_∞ will be a monotonically decreasing function and that, for $|u_\infty| > 10$, the dark soliton converges to a single form. This behavior contrasts with that of the bright screening soliton, for which the narrowest soliton is obtained when the ratio of peak soliton irradiance to background irradiance, is approximately 3. This difference between the dependence of the soliton on its maximum

0146-9592/96/090629-03$10.00/0

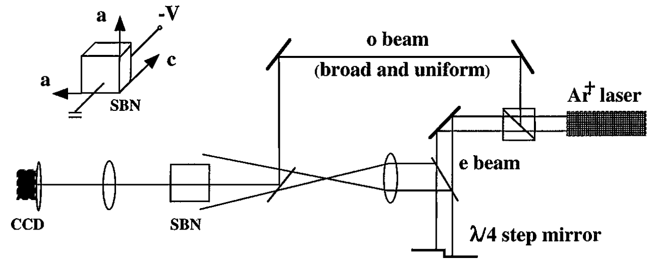

Fig. 1. Experimental setup.

amplitude for bright and dark solitons is unique to photorefractive screening solitons and has no analogy to dark solitons in Kerr media.[12,13] It results from fundamentally different boundary conditions for bright and dark screening solitons: the electron density near the electrodes ($x = \pm \ell/2$) is a function of the light intensity there, u_∞^2, which is zero for bright solitons (and therefore the electron density at $x = \pm\ell/2$ equals that in the dark or that created by background radiation) and is an unknown (u_∞) in the dark-soliton case.[4,5]

To test these predictions for dark solitons it is essential to obtain dark solitons on the background of otherwise uniform beams of infinite extent. If they are not obtained and the dark soliton is generated on finite beams, the boundary conditions resemble those of bright solitons and do not follow the predicted behavior. This is in contrast to the case of dark Kerr solitons on beams of finite extent, for which the finite width of the beam does not substantially affect the dark solitons.[14] This observation poses a challenge that is not required for Kerr solitons: to generate a very narrow dark notch (a few micrometers) in which the transverse phase jumps by π at $x = 0$ on the background of a uniform beam that covers the entire crystal one cannot obtain such a notch by use of a tilted glass plate.[8–10,12,13] We generate this waveform by using a $\lambda/4$ step mirror, made of an InP wafer (reflecting visible light), of which one half is etched to a $\lambda/4$ depth ($\lambda = 488$ nm). We illuminate this mirror by a collimated extraordinarily polarized beam (Fig. 1) and use the reflection, which provides a π phase jump on a 1-cm-wide beam centered at $x = 0$. The reflected notch-bearing beam (typical power ~2 mW) is imaged onto the input face of the SBN:61 crystal, with the narrow direction of the notch parallel to the crystalline c axis and propagating along the a axis. In the experiments of Fig. 4 below (only), we also launch a uniform ordinarily polarized background beam (which simulates the dark irradiance) copropagating with the notch-bearing beam.[6] The input and output faces of the crystal are imaged onto a CCD camera with ±0.75-μm resolution. To observe a dark soliton we apply an external field parallel
notch with polarity opposite to that used for observing bright solitons.[6] In our crystal this field causes a positive index change that, as predicted, has the appropriate sign for trapping a dark soliton.

Typical experimental results showing beam profiles and photographs are presented in Fig. 2. The input notch is 7 μm (FWHM) wide (left) and diffracts (in the absence of external field) to 12 μm (middle) after 5 mm of propagation. V ($= -150$ V) applied between electrodes separated by $\ell = 4.5$ mm traps the notch to a 7-μm width without background illumination. Thus, in accordance with the theoretical prediction,[4] dark screening solitons do not require background illumination, provided that they are generated on an otherwise uniform beam of infinite extent. This contrasts with the claim of Ref. 10 that dark screening solitons require background illumination. We emphasize that, in the absence of background illumination, if we focus the notch-bearing beam so that it does not illuminate the entire crystal the dark soliton appears in quasi-steady state (as observed in Ref. 9) but disappears in the steady state.

To investigate the evolution of the soliton beam, it is desirable to image the soliton beam profile as it propagates throughout the crystal. For this purpose we cut a SBN crystal at 15° with respect to its a axis (Fig. 3, right) and launch the soliton beam. By translating our imaging system laterally we image the output beam after propagation distances that vary between 3.1 and 3.9 mm (keeping a distance from the crystal boundaries) in our 3.7-mm-wide crystal. The soliton profiles at various output planes are shown in Fig. 3 (middle). Within the ±0.75-μm reso-

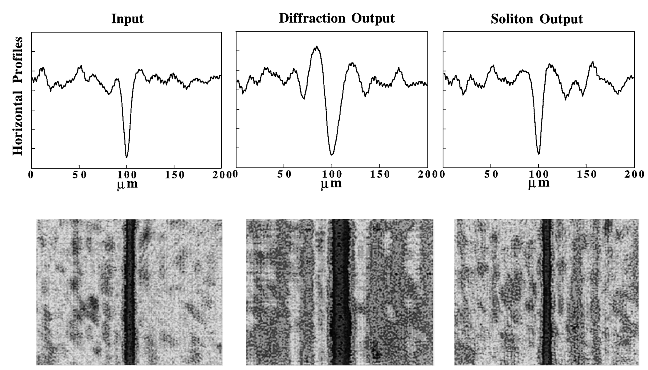

Fig. 2. Beam profiles (above) and photographs (below) of the input beam (left), the normally diffracting output (middle), and the soliton output beams (right) after propagation along a 5-mm SBN crystal.

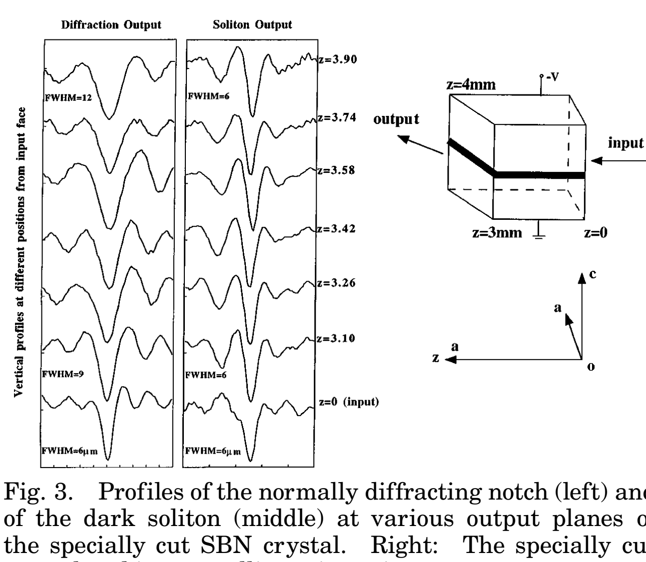

Fig. 3. Profiles of the normally diffracting notch (left) and of the dark soliton (middle) at various output planes of the specially cut SBN crystal. Right: The specially cut crystal and its crystalline orientation.

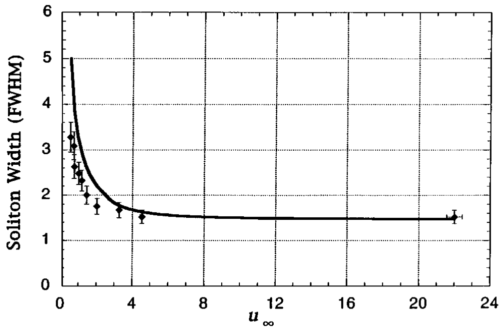

Fig. 4. Theoretical (solid curve) and experimental (error bars) plots of the soliton width in dimensionless units of ξ as a function of the square root of the ratio between the soliton peak intensity and the background plus the dark irradiances (u_∞). The measured soliton width in units of ξ does not change in the range $4.5 \le u_\infty \le 22$.

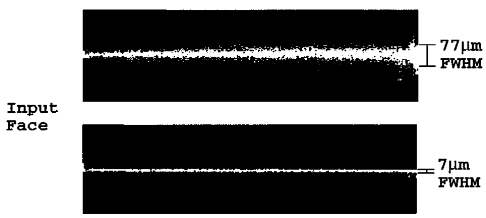

Fig. 5. Top-view photographs of a normally diffracting red beam in a 5-mm SBN crystal (above) and of the red beam guided in the waveguide induced by a dark screening soliton (below).

lution of our imaging system the soliton beam maintains a constant 6-μm (FWHM) profile throughout the entire propagation distance. At zero voltage the beam diffracts from 6 μm at the input face to 9 μm at the shortest (3.1-mm) propagation distance and to 12 μm at the largest (3.9-mm) distance (Fig. 3, left).

Next we test quantitatively the theoretical prediction of a universal relation between the width of the soliton and the ratio of the soliton peak irradiance to the sum of the dark and the background irradiances.[4,5] Measurements of V_π yield $n_b{}^3 r_{\text{eff}} V/(2\ell)$, thus providing $r_{\text{eff}} = r_{33} = 280\,\text{pm/V}$ and $n_b = 2.35$. These measured values, the peak soliton irradiance and the background irradiance, completely determine the solution of Eq. (1). The measured width of the dark soliton in units of ξ as a function of the intensity ratio for a 7-μm-wide dark soliton is shown in Fig. 4 (error bars) and compared with the theoretical result (solid curve). There is good agreement between experiment and theory. As in the theory, we find in our experiments that a dark soliton of a specific width at a given value of intensity ratio exists at a single value of V/ℓ. As predicted, we find that the lowest voltage required for trapping a dark soliton occurs for a soliton intensity much larger than the sum of the dark and background irradiances ($u_\infty{}^2 \gg 1$), where the background illumination is not required. This is the case in spite of small losses that are present in the crystal ($\alpha \approx 0.5\,\text{cm}^{-1}$), because for $u_\infty{}^2 \gg 1$ the soliton width (in ξ units) almost does not change with u_∞ (Fig. 4). For $|u_\infty| \le 1$, because the background and soliton beams have almost identical absorption coefficients, loss does not affect dark-soliton experiments with SBN crystals up to several centimeters long. We also notice that the dark solitons are stable throughout the entire measured range of u_∞, unlike the bright screening solitons that were found[6] to be unstable when the ratio between the soliton peak intensity and the sum of the background and dark irradiances was smaller than unity (in the Kerr limit[4]).

Finally, we launch a second (extraordinarily polarized) beam from a He–Ne laser ($\lambda = 632.8\,\text{nm}$) and guide it in the waveguide induced by the dark screening soliton (similar to guiding experiments with dark quasi-steady-state photorefractive solitons,[11] photovoltaic solitons,[8] and Kerr solitons.[15]) In Fig. 5 we show top-view photographs of the red beam diffracting from 8 to 77 μm FWHM (top) with no voltage applied and of the red beam guided in the waveguide induced by the 7-μm-wide dark soliton (bottom). The guided red beam maintains its width throughout propagation along the 5-mm crystal in steady state (unlike in the transient guidance experiment of Ref. 10).

M. Segev gratefully acknowledges the generous support of the Sloan Fellowship and of Hughes Research Laboratories.

References

1. M. Segev, B. Crosignani, A. Yariv, and B. Fischer, Phys. Rev. Lett. **68,** 923 (1992).
2. G. Duree, J. L. Shultz, G. Salamo, M. Segev, A. Yariv, B. Crosignani, P. DiPorto, E. Sharp, and R. R. Neurgaonkar, Phys. Rev. Lett. **71,** 533 (1993).
3. Observations of steady-state self focusing effects were presented by M. D. Iturbe-Castillo, P. A. Marquez-Aguilar, J. J. Sanchez-Mondragon, S. Stepanov, and V. Vysloukh, Appl. Phys. Lett. **64,** 408 (1994).
4. M. Segev, G. C. Valley, B. Crosignani, P. DiPorto, and A. Yariv, Phys. Rev. Lett. **73,** 3211 (1994); M. Segev, M. Shih, and G. C. Valley, J. Opt. Soc. B **13,** 706 (1996).
5. D. N. Christodoulides and M. I. Carvalho, J. Opt. Soc. Am. B **12,** 1628 (1995).
6. M. Shih, M. Segev, G. C. Valley, G. Salamo, B. Crosignani, and P. DiPorto, Electron. Lett. **31,** 826 (1995); Opt. Lett. **21,** 324 (1996).
7. G. C. Valley, M. Segev, B. Crosignani, A. Yariv, M. M. Fejer, and M. Bashaw, Phys. Rev. A **50,** R4457 (1994).
8. M. Taya, M. Bashaw, M. M. Fejer, M. Segev, and G. C. Valley, Phys. Rev. A **52,** 3095 (1995).
9. G. Duree, M. Morin, G. Salamo, M. Segev, A. Yariv, B. Crosignani, P. DiPorto, and E. Sharp, Phys. Rev. Lett. **74,** 1978 (1995).
10. M. D. Iturbe-Castillo, J. J. Sanchez-Mondragon, S. I. Stepanov, M. B. Klein, and B. A. Wechsler, Opt. Commun. **118,** 515 (1995).
11. M. Morin, G. Duree, G. Salamo, and M. Segev, Opt. Lett. **20,** 2066 (1995).
12. G. A. Swartzlander, D. R. Andersen, J. J. Regan, H. Yin, and A. E. Kaplan, Phys. Rev. Lett. **66,** 1583 (1991).
13. G. R. Allan, S. R. Skinner, D. R. Andersen, and A. L. Smirl, Opt. Lett. **16,** 156 (1991).
14. Y. S. Kivshar and X. Yang, Opt. Commun. **107,** 93 (1994).
15. B. Luther-Davies and Y. Xiaoping, Opt. Lett. **17,** 496 (1992).